

Cosmological constraints on sterile neutrino oscillations from *Planck*

Alan M. Knee,¹ Dagoberto Contreras,^{2,3} Douglas Scott¹

¹Department of Physics & Astronomy

University of British Columbia, Vancouver, BC, V6T 1Z1 Canada

²Department of Physics & Astronomy

University of York, Toronto, ON, M3J 1P3 Canada

³Perimeter Institute for Theoretical Physics, Waterloo, ON, N2L 2Y5 Canada

E-mail: alan.knee@alumni.ubc.ca, dago@yorku.ca, dscott@phas.ubc.ca

Abstract. Both particle physics experiments and cosmological surveys can constrain the properties of sterile neutrinos, but do so with different parameterizations that naturally use different prior information. We present joint constraints on the 3+1 sterile neutrino model oscillation parameters, Δm_{41}^2 and $\sin^2 2\theta$, with uniform priors on those parameters using cosmological data from the *Planck* satellite. Two cases are considered, one where the sterile neutrino mixes with electron neutrinos solely, and another where the sterile neutrino mixes exclusively with muon neutrinos, allowing us to constrain the mixing angles $\sin^2 2\theta_{14}$ and $\sin^2 2\theta_{24}$. We find that when priors are uninformative in the $\Delta m_{41}^2 - \sin^2 2\theta$ parameter space, the *Planck* data show a slight preference for non-zero mass splitting, providing a possible hint of sterile neutrinos; however, we do not claim any detection of sterile neutrinos from this, since the result is prior dependent. We also forecast the sensitivity with which future CMB experiments should be able to probe Δm_{41}^2 and $\sin^2 2\theta$.

1 Introduction

The neutrino sector is still not well understood. In particular the masses and mixing angles of the three Standard Model (SM) neutrinos are still being determined, along with the possibility that there might be additional light leptons. Cosmology has an important role to play here, since the constraints obtained are quite complementary to those coming from particle experiments (see the Review of Particle Physics articles on neutrinos in cosmology and neutrino oscillations in ref. [1]). Models involving more than three types of neutrino have mostly been disfavoured by data from both particle physics and cosmology experiments. However, some neutrino experiments have hinted at the existence of additional neutrino species, and it is often hypothesized these new species, should they exist, are “sterile” neutrinos. Such neutrinos differ from the three standard “active” neutrinos in that they are not charged under the weak interaction and thus lack most of the fundamental interactions experienced by the active neutrinos in the SM. Instead, sterile neutrinos only interact in the cosmological context via gravitation and through mixing with the other neutrinos [2].

The study of sterile neutrinos presents an interesting avenue into new physics beyond the SM. There are many different experiments whose results have hinted at evidence for non-trivial content in the neutrino sector. In perhaps the most prominent example, results from LSND are in tension with other experiments, since there the standard 3-neutrino model do not adequately match the data [3]. The results are well fit with an eV sterile neutrino in a 3+1 neutrino model, although other experiments measuring the same channel exclude this model (see for example ref. [4]). Surprisingly, this anomalous result appears to have been recently corroborated by MiniBooNE,¹ which, combined with the data from LSND, yields an electron excess at the level of $> 6\sigma$ significance [5]. At the present moment the union of all oscillation experimental results seems to be simultaneously at odds with the standard 3-neutrino model and a 3+1 sterile neutrino model, even although some data prefer one over the other. This provides motivation for independently considering the 3+1 sterile neutrino model from a cosmological perspective.

This paper is structured as follows: In section 2 we review the effect that neutrinos have on cosmology and specifically the CMB. Section 3 introduces the specific sterile neutrino that we constrain here. We present our constraints on existing cosmological data in section 4. We forecast how well constraints for a future survey with similar capabilities to the CMB “Stage 4” experiment will perform in section 5. Finally we conclude in section 6.

2 Neutrinos in cosmology and particle physics

Neutrino physics is constrained by the cosmic microwave background (CMB) in terms of two parameters, N_{eff} and Σm_ν . The quantity N_{eff} is the effective number of neutrino species, and *Planck* data are consistent with $N_{\text{eff}} = 3.046$ as predicted by the SM. The SM prediction differs slightly from $N_{\text{eff}} = 3$ due to heating of the neutrinos by electron-positron annihilation during the epoch of neutrino decoupling (see refs. [6–8] for discussion of how the standard value of 3.046 is obtained). Large deviations from this value, on the order of unity, are ruled out by *Planck* at over 99% confidence, but the constraints do allow for small deviations from 3.046 [9]. The second cosmologically relevant quantity, Σm_ν , is the sum of the active neutrino masses. Particle physics experiments have only been able to measure the mass-squared differences

¹Though not consistently for all data channels, see ref. [5].

between neutrino mass states,² so we have the freedom to consider different mass hierarchies. Usually, for cosmology, one assumes the normal hierarchy, which consists of two very light neutrinos, m_1 and m_2 , with the former being the lightest, and a heavier neutrino, m_3 ; however, inverted or degenerate hierarchies are also possible. We will assume the normal hierarchy here (having an inverted hierarchy would strengthen *Planck* constraints on sterile neutrinos), in which there are two massless neutrinos and one massive neutrino with $\Sigma m_\nu = 0.06$ eV [9]. An approximation that is reasonable for cosmological purposes is to take m_1 and m_2 to be massless, leaving Σm_ν to be dominated by m_3 . When one adopts a model that allows for sterile neutrinos, N_{eff} is reinterpreted so that deviations from 3.046 (i.e. $\Delta N_{\text{eff}} = N_{\text{eff}} - 3.046$) indicate an additional degree of freedom associated with the sterile neutrinos [10].

SM neutrinos contribute a cosmological density parameter given by [11]

$$\Omega_\nu = \frac{\rho_\nu}{\rho_{\text{crit}}} \approx \frac{\sum c_i g_i^{3/4} m_i}{94.1 h^2 \text{ eV}} \approx \frac{\sum m_\nu}{93.03 h^2 \text{ eV}}, \quad (2.1)$$

where $h \equiv H_0/(100 \text{ km s}^{-1} \text{ Mpc}^{-1})$ is the reduced Hubble constant. In cosmology, only the three SM neutrinos are included in the mass sum $\sum m_\nu$. The masses m_i represent the active mass eigenstates, c_i is the degeneracy per state, and $g_i = 3.046/3$ is a degeneracy factor that arises because we have $N_{\text{eff}} = 3.046$ distributed among three neutrinos. The three-quarters power comes from the translation between a number density and an energy density within the calculations, and will be elaborated on in a later section. We stress that this relation is only valid in the instantaneous decoupling limit, meaning that the neutrinos are perfectly Fermi-Dirac distributed. In reality, this decoupling is not instantaneous, and heating from electron-positron annihilation, in addition to other quantum-mechanical effects in the early Universe, causes the neutrinos to no longer be exactly Fermi-Dirac, yielding a slightly different factor in the denominator [1, 7]: $\Omega_\nu = \Sigma m_\nu / 93.14 h^2 \text{ eV}$. To be consistent with the *Planck* analysis, we have opted to use the parameterization in eq. 2.1. It is worth pointing out that this means that our approach is not entirely self-consistent, since it is this departure from being perfectly Fermi-Dirac that leads to $N_{\text{eff}} = 3.046$ instead of $N_{\text{eff}} = 3$ in the first place. However, this difference in the second decimal digit is small enough that it will not significantly influence our results.

Sterile neutrinos introduce an additional energy density to the cosmological background, which we can parameterize with $\Omega_{\nu, \text{sterile}}$ as in the *Planck* parameters paper [9]:

$$m_{\nu, \text{sterile}}^{\text{eff}} \equiv 94.1 \Omega_{\nu, \text{sterile}} h^2 \text{ eV}. \quad (2.2)$$

In this case, the total physical neutrino density becomes $\Omega_\nu h^2 = 0.00064 + \Omega_{\nu, \text{sterile}} h^2$, where 0.00064 is the contribution to the physical neutrino density by the three active neutrinos, assuming the standard mass sum $\Sigma m_\nu = 0.06$ eV. Thus, any change from $\Omega_\nu h^2 = 0.00064$ is assumed to be due to sterile neutrinos. This picture is for the simplest case where the sterile neutrinos do not couple with any other neutrino, hence the factor of 94.1 eV.

In particle physics, neutrino properties are mostly constrained through oscillation experiments. The exact masses of neutrinos are unknown, and neutrino experiments instead probe the mass-squared differences Δm_{ij}^2 between two mass eigenstates. For the study of sterile neutrinos we parameterize our model in terms of Δm_{41}^2 , the mass-squared difference

²In terms of the mass of neutrinos, measurements of an effective electron neutrino mass are also possible; nevertheless, the current cosmological constraints have little distinguishing power with respect to the neutrino hierarchy.

between m_4 and the lightest mass state. In the normal hierarchy with $m_1 = 0$, this reduces to a convenient equality: $\Delta m_{41}^2 = m_4^2 - m_1^2 = m_4^2$. Sterile neutrinos, if they exist, are usually considered to be significantly more massive than the three standard species, with a mass closer to the eV scale [12], which has implications for cosmology [2].

For neutrinos, mass states do not correspond uniquely to the flavour states. Instead, the two bases are related through a mixing matrix $U_{\alpha\beta}$. Interpreted in the 3+1 scenario, the mixing matrix is rectangular with $\alpha = e, \mu, \tau$, and $\beta = 1, 2, 3, 4$. The elements of the mixing matrix are products of sines and cosines of the mixing angles θ_{ij} ($i, j = 1, 2, 3, 4$). The flavour states are thus linear combinations of the mass states and vice versa:

$$|\nu_\alpha\rangle = \sum_\beta U_{\alpha\beta}^* |\nu_\beta\rangle. \quad (2.3)$$

Finding stringent constraints on these mixing angles remains an active field of research in experimental particle physics [13]. Neutrino oscillation experiments measure the flux of neutrinos prepared in a preferred flavour at two detectors separated by some large distance, L . The ν_e and ν_μ disappearance searches are concerned with measuring how many neutrinos change flavour as a result of neutrino oscillation, whereas $\nu_e \rightarrow \nu_\mu$ appearance searches measure how many muon neutrinos appear from an initial beam of electron neutrinos. Sterile neutrinos could mix with one or more neutrino flavours; however, in this paper we will only be considering the simpler cases where they mix with a single active species. Therefore, the study of ν_e appearance in ν_μ beams will not be considered here, since analysing such data in the 3+1 scenario would require a 2-flavour oscillation model. The survival probabilities in ν_e and ν_μ disappearance searches are, respectively, given in natural units by [12]

$$P_{ee}^{3+1} = 1 - 4|U_{e4}|^2(1 - |U_{e4}|^2) \sin^2 \left(\frac{\Delta m_{41}^2 L}{4E} \right) = 1 - \sin^2 2\theta_{ee} \sin^2 \left(\frac{\Delta m_{41}^2 L}{4E} \right), \quad (2.4)$$

$$P_{\mu\mu}^{3+1} = 1 - 4|U_{\mu4}|^2(1 - |U_{\mu4}|^2) \sin^2 \left(\frac{\Delta m_{41}^2 L}{4E} \right) = 1 - \sin^2 2\theta_{\mu\mu} \sin^2 \left(\frac{\Delta m_{41}^2 L}{4E} \right), \quad (2.5)$$

where L is the beam length, E is the energy of the neutrinos, and

$$\sin^2 2\theta_{ee} = 4|U_{e4}|^2(1 - |U_{e4}|^2), \quad (2.6)$$

$$\sin^2 2\theta_{\mu\mu} = 4|U_{\mu4}|^2(1 - |U_{\mu4}|^2). \quad (2.7)$$

Using the specific parameterization of the mixing matrix in ref. [12], we have

$$|U_{e4}| = \sin \theta_{14}, \quad (2.8)$$

$$|U_{\mu4}| = \cos \theta_{14} \sin \theta_{24}. \quad (2.9)$$

One therefore finds that in the case where the sterile neutrino only mixes with a muon neutrino (so $\cos \theta_{14} = 1$), the effective sterile neutrino mixing angle reduces to $\sin^2 2\theta_{24} = \sin^2 2\theta_{\mu\mu}$, and if it only mixes with an electron neutrino the mixing is instead determined by $\sin^2 2\theta_{14} = \sin^2 2\theta_{ee}$. Thus, in both situations there is a direct correspondence between sterile neutrino oscillation and either ν_e or ν_μ disappearance, depending on which flavour the sterile neutrino mixes with. We assume $\sin^2 2\theta_{34} = 0$ at all times, in accordance with experimental measurements. More complicated models could in principle have a sterile neutrino that mixes with multiple species, or have more than one sterile species. See ref. [12] for a review covering multiple mixing cases and the 2-sterile neutrino (3+2) scenario.

3 Model

The main complication in comparing cosmological constraints with oscillation measurements arises from the fact that cosmology and neutrino experiments are sensitive to different physical effects and so focus on different parameterizations and priors. In particular, flat priors in one parameter space will not be flat in a different space. We will describe this in general in section 3.1. In refs. [14, 15], a method is developed to express the $(N_{\text{eff}}, m_{\nu, \text{sterile}}^{\text{eff}})$ parameter space in terms of the $(\sin^2 2\theta, \Delta m_{41}^2)$ parameter space and vice versa, which was used in ref. [16], allowing constraints to be directly compared on sterile neutrinos from both the CMB and neutrino-oscillation experiments by converting between parameter spaces. We will explain this conversion in detail in section 3.2. Throughout this paper, we will refer to these two spaces respectively as the “cosmology” and “particle” parameter spaces. Our particular goal is to elaborate on the results of ref. [16] by using a model that has uninformative priors in the particle parameter space. We constrain the particle parameters by way of a Markov chain Monte Carlo analysis of Planck data using **CosmoMC** [17, 18], as well as forecasting how well future experiments could improve upon these constraints. Our cosmological model includes the base- Λ CDM parameters, as well as N_{eff} , and $m_{\nu, \text{sterile}}^{\text{eff}}$, but with a non-flat prior on the cosmology parameters, such that the particle space parameters are initialized with flat priors, which we now describe in more detail.

3.1 Priors

Recall that the purpose of a Markov chain Monte Carlo is to produce a random sample from a distribution $p(\alpha|X)$ known as the posterior, where α is a model parameter and X represents the data. It follows from Bayes’ theorem that

$$p(\alpha|X) = \frac{p(X|\alpha)p(\alpha)}{p(X)} \propto \mathcal{L}(X|\alpha)p(\alpha), \quad (3.1)$$

where $\mathcal{L}(X|\alpha) = p(X|\alpha)$ is the likelihood function and $p(\alpha)$ is the prior, representing an initial belief about the parameter distributions. The posterior is thus proportional to the product of the likelihood and the prior, a relation that forms the basis of Bayesian inference. As the name suggests, the prior represents the state of our knowledge of a parameter *before* considering specific data. Picking a prior is subjective, but it is often chosen to be uninformative, that is it gives no information on the value of the parameter and thus represents our ignorance [19]. In our case we will also be influenced by trying to be consistent with oscillation experiments. In our MCMC calculations, we want to include the particle parameters as model parameters with flat priors, varying them by proxy as we vary N_{eff} and $m_{\nu, \text{sterile}}^{\text{eff}}$ within **CAMB** [20]. However, a uniform distribution in one set of parameters is generally not uniform when transforming to a different set, and thus simply varying N_{eff} and $m_{\nu, \text{sterile}}^{\text{eff}}$ with flat priors and then converting them to the particle space would not yield flat priors in the particle space.

The prior in one parameter space that gives a uniform prior in another space is given by the Jacobian relating the two parameter spaces. This directly follows from the fact that given two probability distributions, e.g. $p_{\text{cosm}}(N_{\text{eff}}, m_{\nu, \text{sterile}}^{\text{eff}})$ and $p_{\text{part}}(\sin^2 2\theta, \Delta m_{41}^2)$, related to each other by a change of variables transformation, the following relation holds:

$$p_{\text{cosm}}(N_{\text{eff}}, m_{\nu, \text{sterile}}^{\text{eff}}) d(N_{\text{eff}}) d(m_{\nu, \text{sterile}}^{\text{eff}}) = p_{\text{part}}(\sin^2 2\theta, \Delta m_{41}^2) d(\sin^2 2\theta) d(\Delta m_{41}^2). \quad (3.2)$$

Therefore if one desires a uniform prior, $p_{\text{part}}(\sin^2 2\theta, \Delta m_{41}^2) = \text{constant}$, on the particle parameters, the prior for the cosmology parameters must satisfy

$$p_{\text{cosm}}(N_{\text{eff}}, m_{\nu, \text{sterile}}^{\text{eff}}) \propto \left\| \frac{\partial(\sin^2 2\theta)}{\partial(N_{\text{eff}})} \frac{\partial(\Delta m_{41}^2)}{\partial(m_{\nu, \text{sterile}}^{\text{eff}})} \right\|, \quad (3.3)$$

which is the Jacobian determinant for this change of variables.

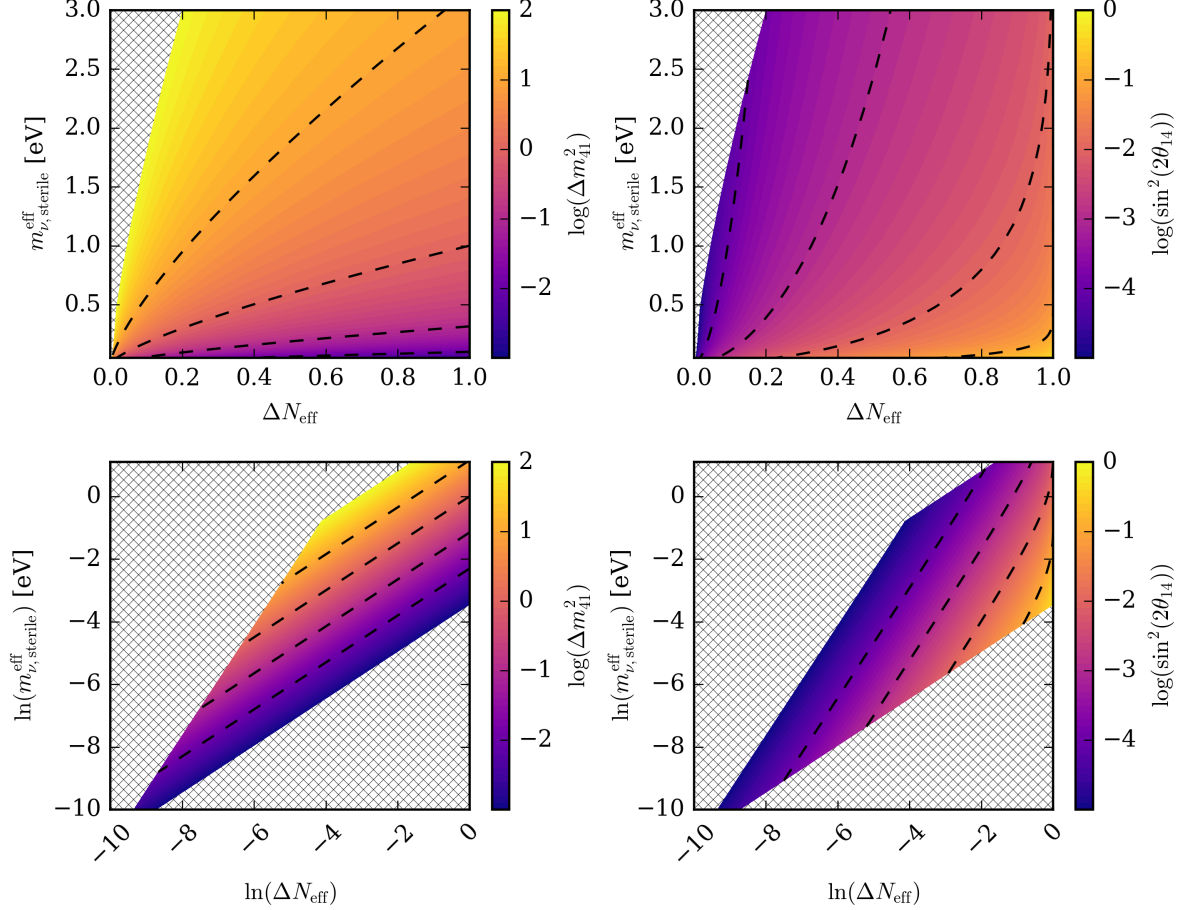


Figure 1. Plots of the LASAGNA output in linear and log spaces of ΔN_{eff} and $m_{\nu, \text{sterile}}^{\text{eff}}$, in which the sterile neutrino mixes with an electron neutrino. The blue regions in the pair of logarithmic plots (lower panels) only intersect with each other at extremely small values of ΔN_{eff} and $m_{\nu, \text{sterile}}^{\text{eff}}$. In linear space, the region of overlap is not even visible and thus sampling it properly is challenging. In log space, this region is greatly expanded and can be well sampled. The hatched regions are excluded by the choice of priors (eq. 3.4). This same set of plots for the case where the sterile neutrino mixes with a muon neutrino looks very similar.

3.2 Parameter-space conversions

Since the particle parameters are not included in the base CosmoMC program, we instead vary N_{eff} and $m_{\nu, \text{sterile}}^{\text{eff}}$ and compute the particle parameters from the chains. To accomplish this, we follow the procedure described in ref. [16] to compute the cosmology parameters on a grid of values for Δm_{41}^2 and $\sin^2 2\theta$ in the ranges

$$10^{-3} \leq \Delta m_{41}^2 \leq 10^2 \text{ eV}^2, \quad 10^{-5} \leq \sin^2 2\theta \leq 1. \quad (3.4)$$

The upper prior limit of 100 eV^2 for the mass splitting is consistent with setting an upper prior limit of $m_4 < 10 \text{ eV}$ on the physical sterile neutrino mass, as done in the Planck Collaboration analysis [9], which is chosen because at masses greater than 10 eV the sterile neutrinos begin to behave like cold dark matter and there is no need to handle them separately. For each point on the grid, we use the code **LASAGNA** [14] to compute N_{eff} and $m_{\nu, \text{sterile}}^{\text{eff}}$, yielding a mapping between the two parameter spaces. **LASAGNA** solves the quantum kinetic equations for sterile neutrino thermalization in the temperature range $1 \leq T \leq 40 \text{ MeV}$, generating discrete values of $x = p/T$ and P_{sterile}^+ , where p is the neutrino momentum, T is the temperature, and P_{sterile}^+ is defined as

$$P_{\text{sterile}}^+ = (P_0 + \bar{P}_0) + (P_z + \bar{P}_z), \quad (3.5)$$

where P_i are the elements of the quantum state vector $\mathbf{P} = (P_0, P_x, P_y, P_z)$ for a particular momentum mode. This output is used to evaluate the integral expression

$$\Delta N_{\text{eff}} = N_{\text{eff}} - 3.046 = \frac{\int dx x^3 (1 + e^x)^{-1} P_{\text{sterile}}^+}{4 \int dx x^3 (1 + e^x)^{-1}} \quad (3.6)$$

by summation. Refs. [14, 15] provide a detailed explanation of the formalism behind the **LASAGNA** code. To obtain an expression for $m_{\nu, \text{sterile}}^{\text{eff}}$, we assume thermally-distributed sterile neutrinos about some temperature T_{sterile} [9, 16]:

$$\Delta N_{\text{eff}} = (T_{\text{sterile}}/T_\nu)^4. \quad (3.7)$$

When $T_\nu = T_{\text{sterile}}$, the sterile neutrinos thermalize at the same temperature as the active neutrinos, resulting in full thermalization of the sterile neutrinos with $\Delta N_{\text{eff}} = 1$. The T^4 proportionality comes from the fact that N_{eff} is parameterizing an energy density. Matter densities, on the other hand, are proportional to T^3 . Using $\Delta m_{41}^2 = m_4^2$, we can compute $m_{\nu, \text{sterile}}^{\text{eff}}$ directly:

$$m_{\nu, \text{sterile}}^{\text{eff}} = (T_{\text{sterile}}/T_\nu)^3 m_4^{\text{thermal}} = (\Delta N_{\text{eff}})^{3/4} m_4^{\text{thermal}} = (\Delta N_{\text{eff}})^{3/4} \sqrt{\Delta m_{41}^2}. \quad (3.8)$$

The **LASAGNA** calculations are quite sensitive to the initial lepton asymmetry L , which we take to be zero. The effects of varying the asymmetry has been studied previously [16], though for simplicity we do not consider it here. Such models may offer additional avenues for studying sterile neutrinos in cosmology. For example, it has been suggested that a large asymmetry could suppress the thermalization of sterile neutrinos in the early Universe, thereby allowing sterile neutrinos to have a large mixing angle without requiring $\Delta N_{\text{eff}} \approx 1$, i.e. complete thermalization [15, 21, 22]. **LASAGNA** supports a single sterile neutrino species that mixes with one active neutrino species. The flavour of the active species can be either an electron neutrino or a muon neutrino, corresponding to the mixing angles θ_{14} and θ_{24} , respectively [12]. We thus have two different cases, each parameterized by a different mixing angle. Both cases are considered in our MCMC runs, allowing us to obtain constraints on either $\sin^2 2\theta_{14}$ or $\sin^2 2\theta_{24}$.

3.3 Sampling

In order to avoid a false detection of sterile neutrinos, it is of critical importance to ensure that the region of parameter space corresponding to small mixing angles and mass splittings is

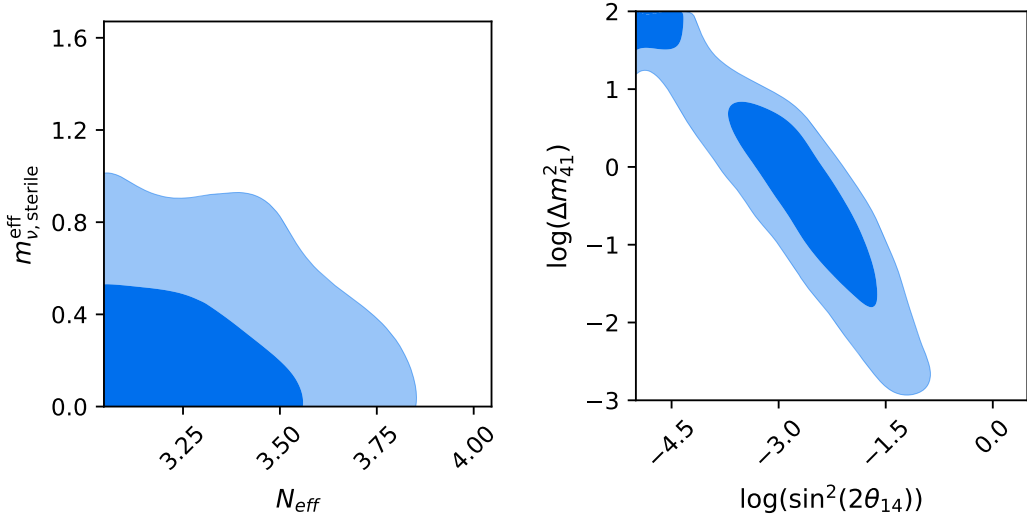


Figure 2. *Left panel:* *Planck* 68% and 95% CL constraints in the cosmology parameter space using *Planck* CMB TT+lowTEB data. Priors are flat in the ranges $3.046 \leq N_{eff} \leq 4.046$ and $0 \leq m_{\nu,sterile}^{eff} \leq 3$ eV. *Right panel:* The procedure explained in section 3.2 is used to calculate the particle parameters from the original cosmology chains. The region of low mass and mixing angle appears to be ruled out, but these constraints are not robust, since this is a result of poor sampling. A solution to this is discussed in section 3.3. Note that here $\log x$ denotes the base 10 logarithm, not the natural logarithm, which we will always write as $\ln x$.

well sampled. Indeed, if we simply compute the particle parameters from N_{eff} and $m_{\nu,sterile}^{eff}$, as was done in figure 2, the region of low mass and mixing angle appears to be ruled out at 95% confidence. However, this is not a genuine detection of high mass, but rather a consequence of the chains being unable to sample from this region. In figure 1, we can see that the region of particle space where both the mixing angle and mass splitting are small is where the darker regions overlap. In the cosmology parameter space, there is practically no overlap at all and thus the Markov chain will be unable to sample this region. To remedy this we switch to a parameterization in terms of $\ln(\Delta N_{eff})$ and $\ln(m_{\nu,sterile}^{eff}) = \ln(\Omega_{\nu,sterile} h^2) + \ln(94.1)$. This effectively scales down the proposal width of the Markov chain when attempting to sample low $\sin^2 2\theta$ and Δm_{41}^2 , giving us much greater resolution at these small scales. One can see in figure 1 that the overlapping region in the logarithmically-scaled plots is clearly visible and thus it should be well sampled when running the MCMC. The prior in this new parameter space that yields flat priors in the particle space is

$$p_{cos}(\ln(\Delta N_{eff}), \ln(m_{\nu,sterile}^{eff})) \propto \left\| \frac{\partial(\sin^2 2\theta) \partial(\Delta m_{41}^2)}{\partial(\ln(\Delta N_{eff}) \partial(\ln(m_{\nu,sterile}^{eff})))} \right\|. \quad (3.9)$$

We compute this Jacobian for each point in the log cosmology parameter space by finding the partial derivatives numerically in each direction and then inverting the determinant of the resulting 2×2 matrix:

$$\mathbb{J} = \begin{pmatrix} \frac{\partial(\ln(\Delta N_{eff}))}{\partial(\sin^2 2\theta)} & \frac{\partial(\ln(\Delta N_{eff}))}{\partial(\Delta m_{41}^2)} \\ \frac{\partial(\ln(m_{\nu,sterile}^{eff}))}{\partial(\sin^2 2\theta)} & \frac{\partial(\ln(m_{\nu,sterile}^{eff}))}{\partial(\Delta m_{41}^2)} \end{pmatrix}. \quad (3.10)$$

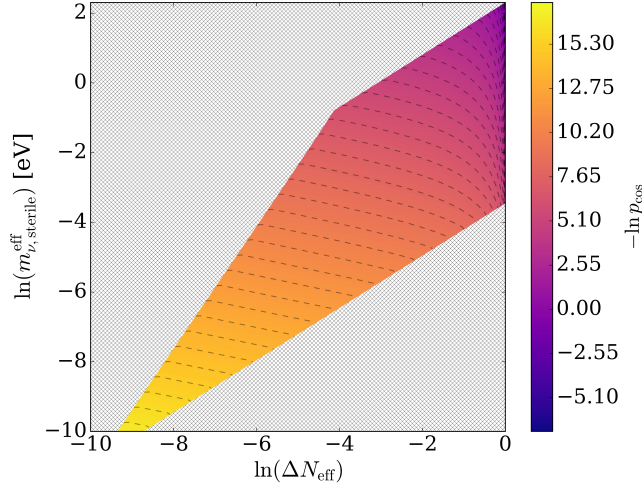


Figure 3. Negative log-values of the (non-normalized) Jacobian used as the prior on $\ln(\Delta N_{\text{eff}})$ and $\ln(m_{\nu,\text{sterile}}^{\text{eff}})$ for the case where the sterile neutrino mixes with an electron neutrino. Large negative values thus correspond to larger probabilities. The probability rises sharply at large $\ln(\Delta N_{\text{eff}})$ and $\ln(m_{\nu,\text{sterile}}^{\text{eff}})$, indicated by the dark blue region in the upper right corner of the plot, and so this region is favoured by the prior. The hatched regions are excluded by the chosen prior ranges for the particle parameter space discussed in section 3.2. The priors for the two different mixing cases (i.e. muon or electron) are practically identical.

The prior is implemented in **CosmoMC** by adding $-\ln p_{\text{cosm}}$ to the negative log-likelihood function ($-\ln \mathcal{L}$) at each chain step, thereby changing the posteriors. We also introduce new prior ranges on the cosmology parameters,

$$-10 \leq \ln(\Delta N_{\text{eff}}) \leq 0, \quad -10 \leq \ln(m_{\nu,\text{sterile}}^{\text{eff}}) \leq \ln 3. \quad (3.11)$$

Since we have switched to logarithmic space, the baseline Λ CDM model with $\Delta N_{\text{eff}} = 0$ and $m_{\nu,\text{sterile}}^{\text{eff}} = 0$ is formally excluded; however, the lower limit of e^{-10} for both of these parameters is still very nearly standard Λ CDM.

The uniform prior on the particle parameters has the largest probabilities at high N_{eff} . This is because, as noted in ref. [9], large mixing angles ($\sin^2 2\theta \geq 0.1$) require near complete thermalization of sterile neutrinos, provided that there is no lepton asymmetry. A uniform prior on the mixing angle will hence strongly favour $\Delta N_{\text{eff}} \approx 1$. Since the default MCMC sampling method in **CosmoMC** is not well suited for dealing with priors with unusual distributions, we run **CosmoChord** alongside **CosmoMC**; this is a nested sampling tool designed to handle any arbitrarily complicated distribution [23, 24].

4 Results

To summarize our approach, we perform a Markov chain Monte Carlo using **CosmoMC** to sample the posteriors for a 2-parameter extension to the base- Λ CDM model,

$$\{\Omega_b h^2, \Omega_c h^2, 100\theta_{\text{MC}}, \tau, \ln(10^{10} A_s), n_s, \ln(\Delta N_{\text{eff}}), \ln(m_{\nu,\text{sterile}}^{\text{eff}})\}, \quad (4.1)$$

using eq. 3.9 as the joint prior on $\ln(\Delta N_{\text{eff}})$ and $\ln(m_{\nu,\text{sterile}}^{\text{eff}})$ with the prior ranges in eq. 3.11, and flat priors on the particle parameter space with the ranges given in eq. 3.4. To see the

effect of the choice of prior on the constraints, we also perform an MCMC run with extended mass priors in the range

$$10^{-5} \leq \Delta m_{41}^2 \leq 10^2 \text{ eV}^2, \quad 10^{-5} \leq \sin^2 2\theta \leq 1. \quad (4.2)$$

The Λ CDM parameters also have flat priors, as usual. The corresponding chains for the particle parameters are calculated from the cosmology parameters using eq. 3.8 and by interpolating over the grid for $\sin^2 2\theta$. We use the normal hierarchy, and assume that the SM neutrinos can be accurately approximated by a single massive species and two massless species with Σm_ν fixed at 0.06 eV. We analyse two distinct mixing cases: one where the sterile species mixes with an electron neutrino; and another where it mixes with a muon neutrino. We compare the results with MCMC runs that have flat priors in the log-cosmology space, as well as with the constraints from neutrino experiments. To be explicit, the data sets used in our MCMC analysis are:

TT+lowTEB power spectra – *Planck* high- ℓ ($30 \leq \ell \leq 2508$) CMB temperature power spectrum combined with low- ℓ ($2 \leq \ell \leq 29$) temperature and LFI polarization data which uses the *Plik* likelihood code [25];

Lensing – *Planck* full-sky lensed CMB *SMICA* reconstruction [26];

BAO – baryon acoustic oscillation data sets DR11CMASS, DR11LOWZ, 6DF, and MGS from the SDSS-III Baryon Oscillation Spectroscopic Survey (BOSS) [27].

4.1 Joint constraints on Δm_{41}^2 and $\sin^2 2\theta_{14}$

In this section we discuss the constraints from our MCMC analysis for the case where the sterile neutrino mixes with an electron neutrino. The top left panel in figure 4 shows the constraints in the particle space, with and without flat priors in this space. With flat priors in the log-cosmology space, *Planck* data rule out large mass splittings and mixing angles at over 90% confidence, and are consistent with no sterile neutrinos (since the posteriors are non-zero at the prior edges). Furthermore, the region of low mixing angle and mass splitting is completely filled, demonstrating that this region of parameter space is being properly sampled by the MCMC.

Assuming flat priors in the particle parameter space changes the constraints considerably. The two sets of constraints appear highly discrepant with each other, which we attribute to volume effects that arise when marginalizing over highly non-Gaussian parameter distributions. Low mixing angles and mass splittings are no longer preferred in all three combinations of likelihood. Low mixing angles are instead only favoured if the sterile neutrino is relatively massive (above about 1 eV²). At first glance it appears as though there is a slight preference for non-zero mass splitting, constraining Δm_{41}^2 above the lower prior limit at 95% confidence (but not at 99%). It is important to emphasize that the 1D Δm_{41}^2 posterior (figure 4) is still slightly non-zero at the lower prior limit. The 68% confidence limits for all relevant

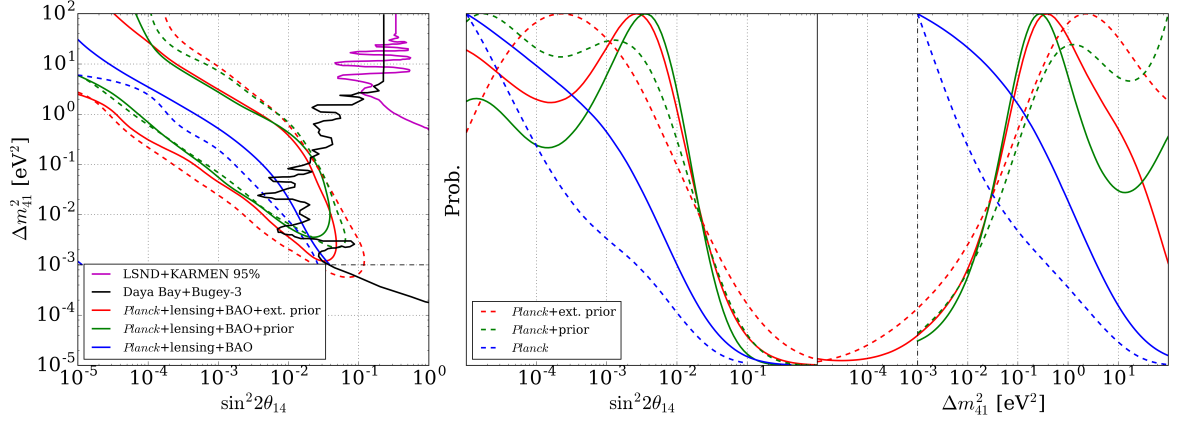


Figure 4. *Left panel:* Joint constraints on the particle parameters for the electron neutrino mixing case, for the three sets of prior. Blue denotes flat priors in the log-cosmology space, green is flat priors in the particle space, and red is flat in the particle space with a lower mass prior limit. The dashed red, green, and blue lines denote constraints from *Planck* TT+lowTEB, and the solid red, green, and blue lines have had BAO and CMB lensing data sets included. For comparison, we have included constraints from some electron neutrino and antineutrino disappearance experiments: a combined KARMEN and LSND analysis [28]; and the more recent Daya Bay/Bugey-3 sterile neutrino search [29]. All limits here are at 90% confidence unless otherwise stated. The region to the right of the black, magenta, and blue curves are excluded, whereas the red and green curves exclude regions outside the contours. The dotted black line denotes the lower mass prior, before it was extended to 10⁻⁵ eV². Note that in the legend, “*Planck*” denotes *Planck* TT+lowTEB data, “prior” denotes flat priors in the particle space given by eq. 3.4, and “ext. prior” denotes flat priors with the lower mass prior. *Right panels:* One-dimensional posteriors for the particle parameters. The line style and colour-coding follows the same scheme as the left panel.

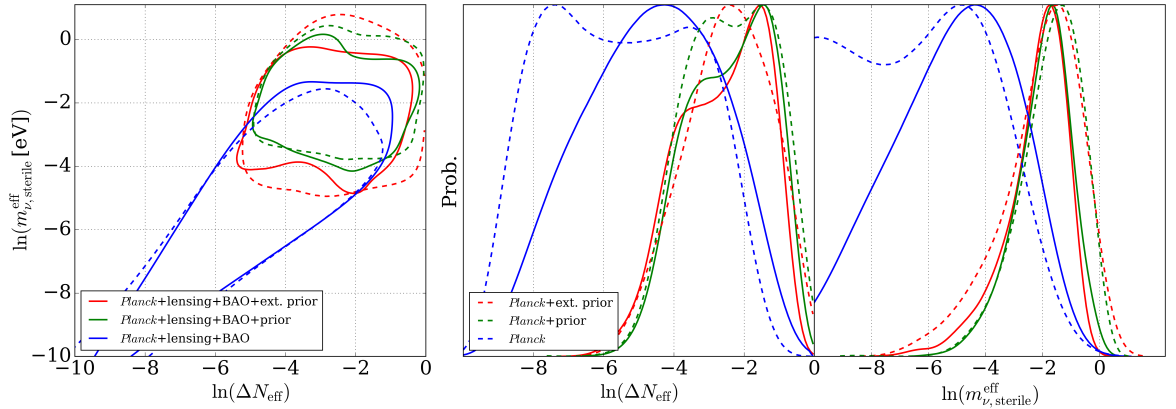


Figure 5. *Left panel:* Joint constraints on the log-cosmology parameters, following the same colour scheme as in figure 4. All constraints are at the 90% confidence level. *Right panel:* One-dimensional posteriors for the log-cosmology parameters.

parameters are shown in table 1. The 95% limits for the particle parameters are

$$\left. \begin{aligned} \Delta m_{41}^2 &> 0.0091 \text{ eV}^2, \\ \sin^2 2\theta_{14} &< 0.025, \end{aligned} \right\} 95\% \text{ TT+lowTEB+prior}, \quad (4.3)$$

$$\left. \begin{aligned} \Delta m_{41}^2 &> 0.011 \text{ eV}^2, \\ \sin^2 2\theta_{14} &< 0.020, \end{aligned} \right\} 95\% \text{ TT+lowTEB+lensing+BAO+prior}. \quad (4.4)$$

$$\left. \begin{aligned} \Delta m_{41}^2 &> 0.0045 \text{ eV}^2, \\ \sin^2 2\theta_{14} &< 0.023, \end{aligned} \right\} 95\% \text{ TT+lowTEB+lensing+BAO+ext.prior}. \quad (4.5)$$

Parameter	TT+lowTEB+prior 68% limits	TT+lowTEB +lensing +BAO+prior 68% limits	TT+lowTEB +lensing +BAO+ext.prior 68% limits
$\Omega_b h^2$	0.02231 ± 0.00028	0.02241 ± 0.00023	0.02237 ± 0.00027
$\Omega_c h^2$	0.1202 ± 0.0023	0.1191 ± 0.0035	0.1192 ± 0.0030
$100\theta_{\text{MC}}$	1.04063 ± 0.00051	1.04088 ± 0.00046	1.04090 ± 0.00044
τ	0.084 ± 0.021	0.075 ± 0.016	0.073 ± 0.015
$\ln(10^{10} A_s)$	3.106 ± 0.042	3.085 ± 0.033	3.080 ± 0.031
n_s	0.968 ± 0.010	0.9729 ± 0.0079	0.9718 ± 0.0069
ΔN_{eff}	$0.09^{+0.31}_{-0.060}$	$0.09^{+0.32}_{-0.057}$	$0.074^{+0.12}_{-0.074}$
$m_{\nu, \text{sterile}}^{\text{eff}} [\text{eV}]$	$0.18^{+0.51}_{-0.10}$	$0.14^{+0.28}_{-0.071}$	$0.11^{+0.14}_{-0.065}$
$\Delta m_{41}^2 [\text{eV}^2]$	> 0.35	> 0.18	$0.57^{+13}_{-0.52}$
$\sin^2 2\theta_{14}$	< 0.0020	< 0.0031	< 0.0028
$H_0 [\text{km s}^{-1} \text{ Mpc}^{-1}]$	67.4 ± 1.5	68.34 ± 0.95	68.19 ± 0.85
σ_8	0.802 ± 0.030	0.798 ± 0.020	0.780 ± 0.018

Table 1. 68% CL parameter constraints in the 2-parameter extension to the base- Λ CDM model for the electron-neutrino-mixing case along with relevant derived parameters. The constraints on $\ln(\Delta N_{\text{eff}})$ and $\ln(m_{\nu, \text{sterile}}^{\text{eff}})$ have been converted to linear values for ease of interpretation here.

The addition of lensing and BAO to the TT+lowTEB power spectrum data tightens the mass constraint up to $\Delta m_{41}^2 > 0.011 \text{ eV}^2$. This offers a possible hint of sterile neutrinos, but given the slightly non-zero mass posterior at low masses, these constraints are not strong enough to claim a detection. Lowering the mass prior also notably affects the constraints. In particular, it brings the lower bound on the mass splitting down to $\Delta m_{41}^2 > 0.00045 \text{ eV}^2$ from $\Delta m_{41}^2 > 0.011 \text{ eV}^2$, and so there appears to be some prior dependence in the constraints. This further suggests that this apparent preference for non-zero mass is not a detection, but something that is at least in part driven by the choice of prior. Adding flat priors in the particle space leads to a weak preference for moderate mixing angles in the range 0.001–0.01, as shown by the emergence of a peak covering this range in the 1D $\sin^2 2\theta_{14}$ posterior; however the constraint remains as an upper limit of $\sin^2 2\theta_{14} < 0.020$ when the full data set is used. Since $\theta_{41} = 0$ is not ruled out, we have not excluded the case where the sterile neutrinos do not engage in any mixing with other neutrinos.

There are stronger constraints on the log-cosmology parameters, as shown in the left panel of figure 5. With flat priors in the log-cosmology space, the posteriors run up against the lower prior edges, consistent with no sterile neutrinos. Switching to flat priors in the particle parameter space leads to upper and lower constraints on $\ln(\Delta N_{\text{eff}})$ and $\ln(m_{\nu, \text{sterile}}^{\text{eff}})$, though it is important to keep in mind that we are not uninformative in this space due to the imposed Jacobian prior. These constraints nonetheless fall well within the $(N_{\text{eff}}, m_{\nu, \text{sterile}}^{\text{eff}})$ confidence limits of the Planck Collaboration analysis [9]. Fully thermalized sterile neutrinos with $\Delta N_{\text{eff}} = 1$ remain excluded at 90% confidence when combining lensing and BAO data with the TT+lowTEB power spectrum. This suggests that the sterile neutrinos would have to be incompletely thermalized in the early Universe through some sort of cosmological suppression mechanism. At first it may seem counter-intuitive that relatively small $m_{\nu, \text{sterile}}^{\text{eff}}$ are constrained, while Δm_{41}^2 is unconstrained at the upper end. However, because the effective mass depends on both the effective number of sterile species and its physical mass, one can have a small effective mass and a large physical mass if this is compensated by a small effective number of species.

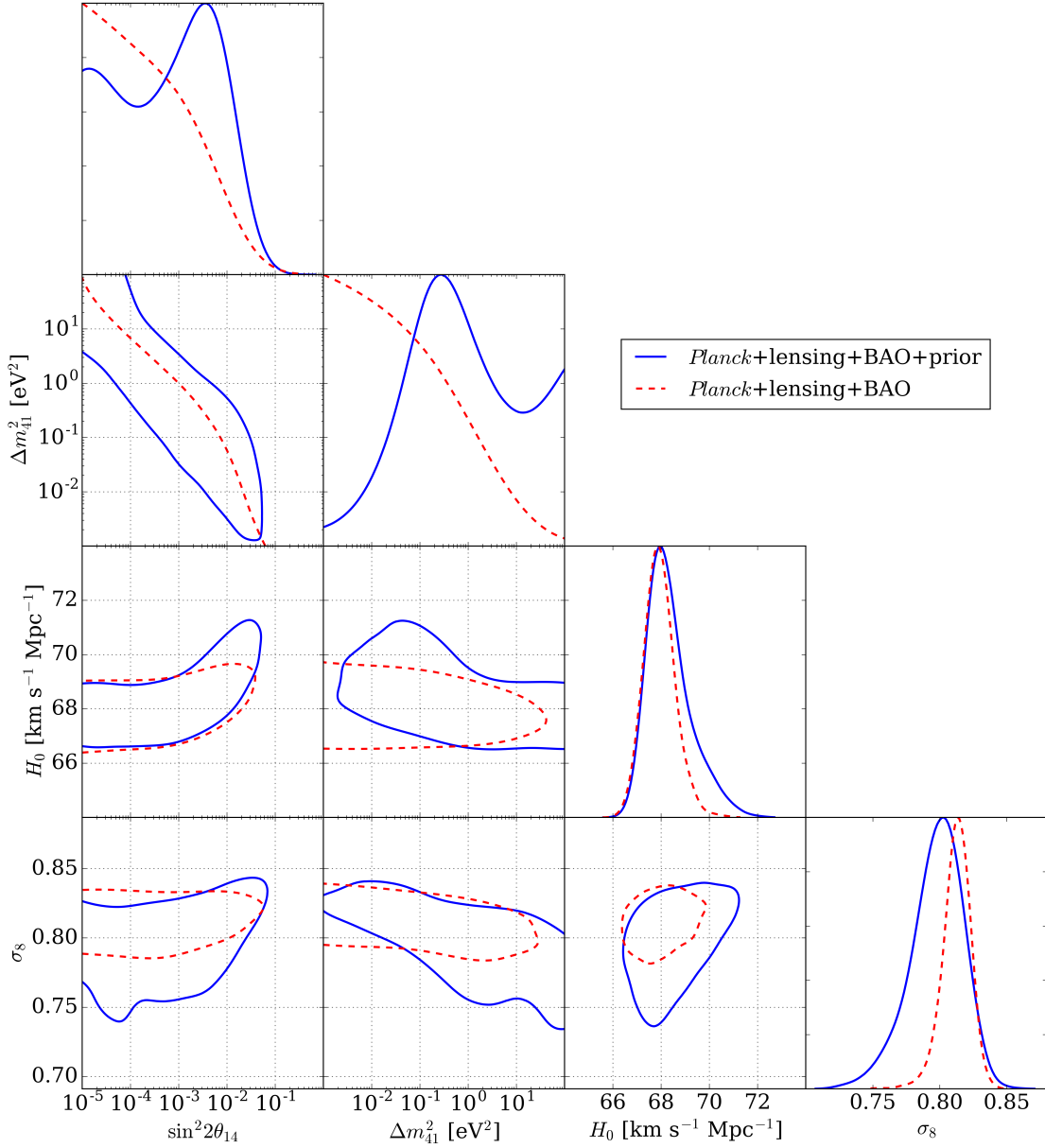


Figure 6. Covariances between the particle parameters, H_0 , and σ_8 for the electron neutrino mixing case. The solid blue lines are the results with flat priors in the particle space, and the dashed red lines are for flat priors in the log-cosmology space. The full data set of *Planck* TT+lowTEB power spectra, lensing, and BAO is used. Limits are at 95% confidence.

Since a great deal of attention has been given to possible tensions between CMB measurements and several low-redshift parameter constraints, it is worth examining how sterile neutrinos might affect these tensions. Figure 6 shows that the switch to flat priors in the particle space has little effect on the correlation between $\sin^2 2\theta_{14}$ and the Hubble parameter, H_0 , except beyond $\sin^2 2\theta_{14} > 0.01$, where increasing the mixing angle starts to increase H_0 . A high mixing angle thus appears to drive an increase in the expansion rate of the Universe, and may help to relieve the current H_0 tension [30]. Flat priors in the particle space also

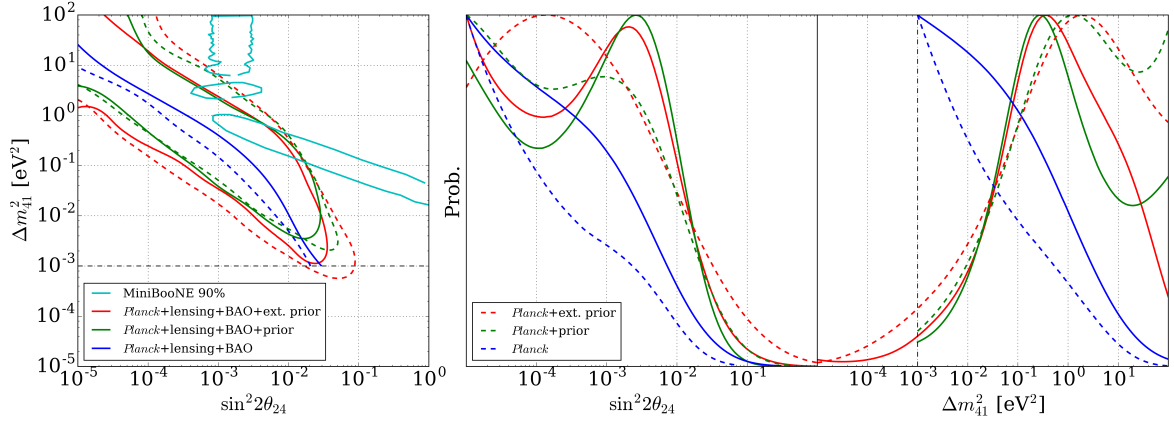


Figure 7. *Left panel:* Joint constraints on the particle parameters for the muon neutrino mixing case, for the three sets of priors. Blue denotes flat priors in the log-cosmology space, green is flat priors in the particle space, and red is flat in the particle space with a lower mass prior limit. The dashed red, green, and blue lines denote constraints from *Planck* TT+lowTEB, and the solid red, green, and blue lines have had BAO and CMB lensing data sets included. For comparison, we have included constraints from a MiniBooNE electron neutrino and antineutrino appearance experiment [5]. All limits are at 90% confidence unless otherwise stated. The regions to the right of the blue curves are excluded, whereas the red, green, and cyan curves exclude regions outside the contours. The dotted black lines denote the lower mass prior, before it was extended to 10⁻⁵ eV². Note that in the legend, “*Planck*” denotes *Planck* TT+lowTEB data, “prior” denotes flat priors in the particle space given by eq. 3.4, and “ext.prior” denotes flat priors with the lower mass prior. *Right panels:* One-dimensional posteriors for the particle parameters. The line style and color-coding follows the same scheme as in the left panel.

make lower amplitude parameter σ_8 marginally more favourable. There is a very slight correlation between $\sin^2 2\theta_{14}$ and σ_8 , with larger mixing angles allowing a slight increase in σ_8 . This behaviour is mirrored in the covariances with Δm_{41}^2 . Large masses do not significantly modify H_0 , but at lower masses the confidence region for H_0 greatly spreads out, with there being a slight preference for larger H_0 at low masses. Large masses also prefer smaller σ_8 , but this increases as the mass decreases. Flat priors in the particle space weaken the constraints on H_0 and σ_8 , which have wider posteriors compared to the MCMC run with flat priors in the log-cosmology space.

4.2 Joint constraints on Δm_{41}^2 and $\sin^2 2\theta_{24}$

As mentioned previously, having the sterile neutrino mix with a muon neutrino, as opposed to an electron neutrino, makes very little difference to the calculation of ΔN_{eff} and $m_{\nu, \text{sterile}}^{\text{eff}}$. The constraint on $\sin^2 2\theta_{24}$ will be very similar to the constraint on $\sin^2 2\theta_{14}$, and so most of what has been said about the latter will be applicable to the former. Since the Jacobians for the two cases are quite similar, the ratio of the Jacobians is approximately constant, and so we can obtain the corresponding constraints for the muon neutrino mixing case by multiplying the likelihoods from the previous set of chains by this ratio. The 95% limits for the particle

parameters for the muon neutrino mixing case are

$$\left. \begin{aligned} \Delta m_{41}^2 &> 0.0088 \text{ eV}^2, \\ \sin^2 2\theta_{24} &< 0.035, \end{aligned} \right\} 95\% \text{ TT+lowTEB+prior}, \quad (4.6)$$

$$\left. \begin{aligned} \Delta m_{41}^2 &> 0.010 \text{ eV}^2, \\ \sin^2 2\theta_{24} &< 0.015, \end{aligned} \right\} 95\% \text{ TT+lowTEB+lensing+BAO+prior}. \quad (4.7)$$

$$\left. \begin{aligned} \Delta m_{41}^2 &> 0.0043 \text{ eV}^2, \\ \sin^2 2\theta_{24} &< 0.017, \end{aligned} \right\} 95\% \text{ TT+lowTEB+lensing+BAO+ext.prior}. \quad (4.8)$$

5 Forecasting

The only way to determine whether these prior dependent are a sign of new physics is to obtain better data. Several future CMB experiments, like CMB-S4 [31, 32], aim to improve the constraints on cosmological neutrinos. Fisher matrix methods are commonly used by cosmologists to predict the precision with which these future experiments could measure neutrino parameters, and in this section we proceed to apply these techniques to forecast sterile neutrino constraints in the particle parameter space.

To forecast constraints from the CMB, one must first calculate the Fisher matrix for a given fiducial (baseline) model. For an n -parameter model, the Fisher matrix is a square $n \times n$ matrix that fully encodes all the information from the CMB. Calculating Fisher matrices normally involves finding the first moment of the Hessian of the log-likelihood function for the fiducial model. However, by assuming Gaussian perturbations in the CMB temperature and polarization anisotropies, the Fisher matrix for the CMB can be rewritten as [33]

$$F_{ij} = \sum_{\ell} \sum_{XY} \frac{\partial C_{\ell}^X}{\partial p_i} (\mathbb{C})_{XY}^{-1} \frac{\partial C_{\ell}^Y}{\partial p_j} \quad (5.1)$$

where $X = T, E, C$, respectively, denote the temperature, E -mode polarization, and temperature-polarization correlation terms, p_i are the model parameters, and \mathbb{C} is the covariance matrix

$$\mathbb{C} = \begin{pmatrix} (\mathbb{C})_{TT} & (\mathbb{C})_{TE} & (\mathbb{C})_{TC} \\ (\mathbb{C})_{TE} & (\mathbb{C})_{EE} & (\mathbb{C})_{EC} \\ (\mathbb{C})_{TC} & (\mathbb{C})_{EC} & (\mathbb{C})_{CC} \end{pmatrix}. \quad (5.2)$$

Here we have ignored the primordial B -modes, since they are yet to be well measured and are likely far too weak for our model to be sensitive to them [34]. The Cramer-Rao inequality then places upper bounds on the errors for the model parameters, $\sigma_i \leq \sqrt{F_{ii}^{-1}}$. The inverse of the Fisher matrix is used, since all the model parameters are allowed to float. If one does not use the inverse here, then the errors correspond to the case where all the other parameters are fixed. The derivatives of the C_{ℓ} s in eq. 5.1 are taken about the chosen fiducial model.

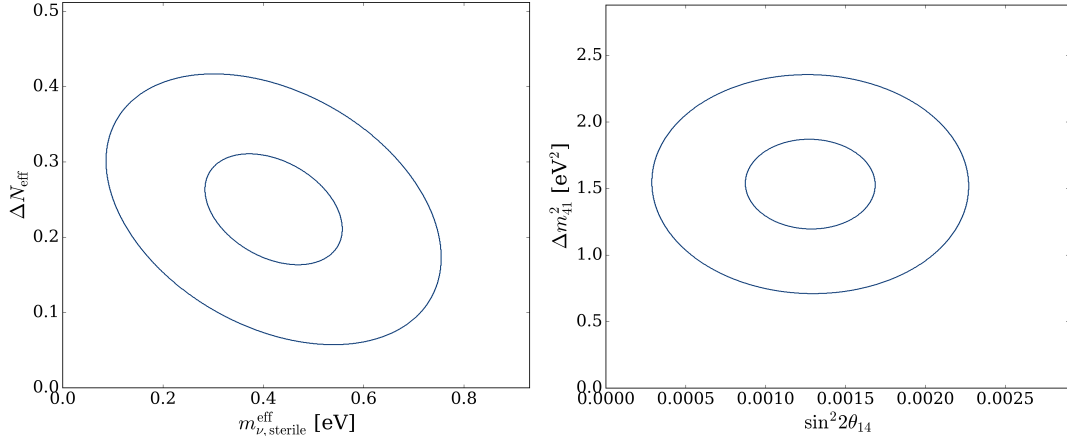


Figure 8. Confidence ellipses in the $\Delta N_{\text{eff}} - m_{\nu, \text{sterile}}^{\text{eff}}$ and $\Delta m_{41}^2 - \sin^2 2\theta_{14}$ planes for an experiment resembling CMB-S4, with $f_{\text{sky}} = 0.4$, a 1-arcmin beam, and noise levels in T and E of $1 \mu\text{K-arcmin}$ and $\sqrt{2} \mu\text{K-arcmin}$, respectively [31]. The covariance matrix for the full $TT + TE + EE$ spectrum is used. The fiducial points are $(\Delta m_{41}^2, \sin^2 2\theta) = (1.5 \text{ eV}^2, 0.0013)$, and $(\Delta N_{\text{eff}}, m_{\nu, \text{sterile}}^{\text{eff}}) = (0.24, 0.42 \text{ eV})$. The derivatives are computed about the log-cosmology parameters, so the uncertainties shown here have been converted to linear values. The contours show the joint 68% and 95% uncertainties in the parameters.

Accounting for instrumental noise, the elements of the covariance matrix are [33]

$$(\mathbb{C})_{TT} = \frac{2}{(2\ell + 1)f_{\text{sky}}} (C_\ell^{TT} + w_T^{-1} B_\ell^{-2})^2, \quad (5.3)$$

$$(\mathbb{C})_{TE} = \frac{2}{(2\ell + 1)f_{\text{sky}}} (C_\ell^{TE})^2, \quad (5.4)$$

$$(\mathbb{C})_{TC} = \frac{2}{(2\ell + 1)f_{\text{sky}}} C_\ell^{TE} (C_\ell^{TT} + w_T^{-1} B_\ell^{-2}), \quad (5.5)$$

$$(\mathbb{C})_{EE} = \frac{2}{(2\ell + 1)f_{\text{sky}}} (C_\ell^{EE} + w_P^{-1} B_\ell^{-2})^2, \quad (5.6)$$

$$(\mathbb{C})_{EC} = \frac{2}{(2\ell + 1)f_{\text{sky}}} C_\ell^{TE} (C_\ell^{EE} + w_P^{-1} B_\ell^{-2}), \quad (5.7)$$

$$(\mathbb{C})_{CC} = \frac{1}{(2\ell + 1)f_{\text{sky}}} [(C_\ell^{TE})^2 + (C_\ell^{TT} + w_T^{-1} B_\ell^{-2})(C_\ell^{EE} + w_P^{-1} B_\ell^{-2})], \quad (5.8)$$

The constants w_T and w_P are the inverse squares of the detector noise level over a steradian patch of the sky for T and E , f_{sky} is the fraction of the sky being observed, and

$$B_\ell^2 = \exp\left(\frac{-\ell(\ell + 1)\theta_{\text{beam}}^2}{8 \ln 2}\right) \quad (5.9)$$

is the beam window function, where θ_{beam} is the full-width, half-maximum beam angle [33]. The noise terms vanish in the limit of zero detector noise, $w_T, w_P \rightarrow \infty$, yielding the covariance matrix for the noise-free case.

We use CAMB [20] to compute the power spectra for finding the derivatives of the C_ℓ s with respect to each parameter for the model presented in section 4. The derivatives with respect to the particle parameters are computed from the derivatives with respect to $\ln(\Delta N_{\text{eff}})$ and

$\ln(m_{\nu,\text{sterile}}^{\text{eff}})$ and then applying the chain rule. We then calculate the Fisher matrix for an experiment with noise levels and beam settings similar to those of CMB-S4, and plot the confidence ellipses in figure 8.

6 Conclusions

We have used *Planck* data to obtain cosmological constraints on the sterile-neutrino oscillation parameters: the squared mass splitting Δm_{41}^2 ; and the mixing angles $\sin^2 2\theta_{14}$ and $\sin^2 2\theta_{24}$, corresponding to two different models where a single sterile neutrino species mixes with an electron neutrino or a muon neutrino. The posteriors were inferred using an MCMC analysis of *Planck* CMB power spectra, lensing, and BAO data, where our model consists of the six Λ CDM parameters plus $\ln(\Delta N_{\text{eff}})$ and $\ln(m_{\nu,\text{sterile}}^{\text{eff}})$, which were used to vary Δm_{41}^2 and $\sin^2 2\theta$ by proxy. We compared results that have flat priors in the log-cosmology space with results which had flat priors in the particle parameter space, which was accomplished by imposing the Jacobian of the change of variables transformation between the two parameter spaces as the prior in the log-cosmology space. The *Planck* data show a slight preference for non-zero mass splitting when priors are flat in the particle space in the range $10^{-3} \leq \Delta m_{41}^2 \leq 10^2 \text{ eV}^2$, $10^{-5} \leq \sin^2 2\theta \leq 1$, yielding $\Delta m_{41}^2 > 0.011 \text{ eV}^2$ and $\sin^2 2\theta_{14} < 0.020$ at 95% confidence for the TT+lowTEB+lensing+BAO data set in the neutrino mixing angle case. The constraints in the muon mixing angle case were found to be $\Delta m_{41}^2 > 0.010 \text{ eV}^2$ and $\sin^2 2\theta_{24} < 0.015$ at 95% confidence.

We examined possible prior dependence in the constraints by extending the lower limit on the mass-splitting prior down to 10^{-5} eV^2 ; this changes the lower bound on the mass splitting, which is $\Delta m_{41}^2 > 0.0045$ and $\Delta m_{41}^2 > 0.0043$ for the electron- and muon-neutrino mixing cases, respectively. Furthermore, the 1D posteriors for the mass-splitting remain slightly non-zero for both cases when log-scales are used. This fact, combined with the apparent prior dependence, indicates no robust detection of sterile neutrinos. We caution that it might be possible to be mislead into drawing strong conclusions based on a particular choice of prior (even if that is implicit in the choice of parameter space). Better cosmology data will enable us to tell whether there is a hint of sterile neutrinos, independent of the prior choice.

Acknowledgments

This work was supported by the Natural Sciences and Engineering Research Council of Canada (www.nserc-crsng.gc.ca). Computing resources were provided by WestGrid (www.westgrid.ca) and Compute Canada/Calcul Canada (www.computecanada.ca). Our main results were obtained using the codes LASAGNA, CAMB, and CosmoMC. We also thank Julien Lesgourgues for helpful discussions on neutrino physics.

References

- [1] PARTICLE DATA GROUP collaboration, M. Tanabashi et al., *Review of Particle Physics*, *Phys. Rev. D* **D98** (2018) 030001.
- [2] K. N. Abazajian et al., *Light Sterile Neutrinos: A White Paper*, [1204.5379](#).
- [3] LSND collaboration, A. Aguilar-Arevalo et al., *Evidence for neutrino oscillations from the observation of anti-neutrino(electron) appearance in a anti-neutrino(muon) beam*, *Phys. Rev. D* **D64** (2001) 112007 [[hep-ex/0104049](#)].

- [4] OPERA collaboration, N. Agafonova et al., *Final results of the search for $\nu_\mu \rightarrow \nu_e$ oscillations with the OPERA detector in the CNGS beam*, *JHEP* **06** (2018) 151 [[1803.11400](#)].
- [5] MINIBOONE collaboration, A. A. Aguilar-Arevalo et al., *Significant Excess of ElectronLike Events in the MiniBooNE Short-Baseline Neutrino Experiment*, [1805.12028](#).
- [6] G. Mangano, G. Miele, S. Pastor and M. Peloso, *A Precision calculation of the effective number of cosmological neutrinos*, *Phys. Lett. B* **534** (2002) 8 [[astro-ph/0111408](#)].
- [7] G. Mangano, G. Miele, S. Pastor, T. Pinto, O. Pisanti and P. D. Serpico, *Relic neutrino decoupling including flavour oscillations*, *Nuclear Physics B* **729** (2005) 221 [[hep-ph/0506164](#)].
- [8] P. F. de Salas and S. Pastor, *Relic neutrino decoupling with flavour oscillations revisited*, *JCAP* **1607** (2016) 051 [[1606.06986](#)].
- [9] PLANCK collaboration, *Planck 2015 results. XIII. Cosmological parameters*, *Astron. Astrophys.* **594** (2016) A13 [[1502.01589](#)].
- [10] J. Lesgourgues and S. Pastor, *Massive neutrinos and cosmology*, *Phys. Rept.* **429** (2006) 307 [[astro-ph/0603494](#)].
- [11] A. Lewis, “CAMB Notes.” <https://cosmologist.info/notes/CAMB.pdf>, 2014.
- [12] J. Kopp, P. A. N. Machado, M. Maltoni and T. Schwetz, *Sterile Neutrino Oscillations: The Global Picture*, *JHEP* **05** (2013) 050 [[1303.3011](#)].
- [13] V. Barger, D. Marfatia and K. Whisnant, *The Physics of Neutrinos*. Princeton University Press, 2012.
- [14] S. Hannestad, R. S. Hansen and T. Tram, *Can active-sterile neutrino oscillations lead to chaotic behavior of the cosmological lepton asymmetry?*, *JCAP* **1304** (2013) 032 [[1302.7279](#)].
- [15] S. Hannestad, I. Tamborra and T. Tram, *Thermalisation of light sterile neutrinos in the early universe*, *JCAP* **1207** (2012) 025 [[1204.5861](#)].
- [16] S. Bridle, J. Elvin-Poole, J. Evans, S. Fernandez, P. Guzowski and S. Soldner-Rembold, *A Combined View of Sterile-Neutrino Constraints from CMB and Neutrino Oscillation Measurements*, *Phys. Lett. B* **764** (2017) 322 [[1607.00032](#)].
- [17] A. Lewis, *Efficient sampling of fast and slow cosmological parameters*, *Phys. Rev. D* **87** (2013) 103529 [[1304.4473](#)].
- [18] A. Lewis and S. Bridle, *Cosmological parameters from CMB and other data: A Monte Carlo approach*, *Phys. Rev. D* **66** (2002) 103511 [[astro-ph/0205436](#)].
- [19] P. C. Gregory, *Bayesian Logical Data Analysis for the Physical Sciences*. Cambridge University Press, 2005.
- [20] A. Lewis, A. Challinor and A. Lasenby, *Efficient computation of CMB anisotropies in closed FRW models*, *Astrophys. J.* **538** (2000) 473 [[astro-ph/9911177](#)].
- [21] N. Saviano, A. Mirizzi, O. Pisanti, P. D. Serpico, G. Mangano and G. Miele, *Multi-momentum and multi-flavour active-sterile neutrino oscillations in the early universe: role of neutrino asymmetries and effects on nucleosynthesis*, *Phys. Rev. D* **87** (2013) 073006 [[1302.1200](#)].
- [22] S. Gariazzo, C. Giunti and M. Laveder, *Cosmological Invisible Decay of Light Sterile Neutrinos*, [1404.6160](#).
- [23] W. J. Handley, M. P. Hobson and A. N. Lasenby, *PolyChord: nested sampling for cosmology*, *Mon. Not. Roy. Astron. Soc.* **450** (2015) L61 [[1502.01856](#)].
- [24] W. J. Handley, M. P. Hobson and A. N. Lasenby, *POLYCHORD: next-generation nested sampling*, *Mon. Not. Roy. Astron. Soc.* **453** (2015) 4384 [[1506.00171](#)].
- [25] PLANCK collaboration, *Planck 2015 results. XI. CMB power spectra, likelihoods, and robustness of parameters*, *Astron. Astrophys.* **594** (2016) A11 [[1507.02704](#)].

- [26] PLANCK collaboration, P. A. R. Ade et al., *Planck 2015 results. XV. Gravitational lensing*, *Astron. Astrophys.* **594** (2016) A15 [[1502.01591](#)].
- [27] BOSS collaboration, L. Anderson et al., *The clustering of galaxies in the SDSS-III Baryon Oscillation Spectroscopic Survey: baryon acoustic oscillations in the Data Releases 10 and 11 Galaxy samples*, *Mon. Not. Roy. Astron. Soc.* **441** (2014) 24 [[1312.4877](#)].
- [28] J. M. Conrad and M. H. Shaevitz, *Limits on Electron Neutrino Disappearance from the KARMEN and LSND ν_e - Carbon Cross Section Data*, *Phys. Rev.* **D85** (2012) 013017 [[1106.5552](#)].
- [29] MINOS, DAYA BAY collaboration, P. Adamson et al., *Limits on Active to Sterile Neutrino Oscillations from Disappearance Searches in the MINOS, Daya Bay, and Bugey-3 Experiments*, *Phys. Rev. Lett.* **117** (2016) 151801 [[1607.01177](#)].
- [30] A. G. Riess et al., *A 2.4% Determination of the Local Value of the Hubble Constant*, *Astrophys. J.* **826** (2016) 56 [[1604.01424](#)].
- [31] CMB-S4 collaboration, K. N. Abazajian et al., *CMB-S4 Science Book, First Edition*, [1610.02743](#).
- [32] M. H. Abitbol, Z. Ahmed, D. Barron, R. Basu Thakur, A. N. Bender, B. A. Benson et al., *CMB-S4 Technology Book, First Edition, ArXiv e-prints* (2017) [[1706.02464](#)].
- [33] D. J. Eisenstein, W. Hu and M. Tegmark, *Cosmic complementarity: Joint parameter estimation from CMB experiments and redshift surveys*, *Astrophys. J.* **518** (1999) 2 [[astro-ph/9807130](#)].
- [34] D. Scott, D. Contreras, A. Narimani and Y.-Z. Ma, *The information content of cosmic microwave background anisotropies*, *JCAP* **1606** (2016) 046 [[1603.03550](#)].